Sleep Medicine 53 (2019) 51–59

Contents lists available at ScienceDirect

Sleep Medicine

journal homepage: www.elsevier.com/locate/sleep

Original Article

White matter structural differences in OSA patients experiencing residual daytime sleepiness with high CPAP use: a non-Gaussian diffusion MRI study

Jiaxuan Zhang [a, b], Terri E. Weaver [f, h, **, 1], Zheng Zhong [a, d], Robyn A. Nisi [f], Kelly R. Martin [f], Alana D. Steffen [g], M. Muge Karaman [a, d], Xiaohong Joe Zhou [a, c, d, e, *, 1]

[a] Center for MR Research, University of Illinois, Chicago, IL, USA
[b] Department of Radiology, Tongji Hospital, Huazhong University of Science and Technology, Wuhan, China
[c] Department of Radiology, College of Medicine, University of Illinois, Chicago, IL, USA
[d] Department of Bioengineering, College of Medicine, University of Illinois, Chicago, IL, USA
[e] Department of Neurosurgery, College of Medicine, University of Illinois, Chicago, IL, USA
[f] Department of Biobehavioral Health Science, University of Illinois, Chicago, IL, USA
[g] Department of Health Systems Science, University of Illinois, Chicago, IL, USA
[h] Center for Sleep and Health, College of Nursing, University of Illinois, Chicago, IL, USA

ARTICLE INFO

Article history:
Received 28 February 2018
Received in revised form
19 August 2018
Accepted 20 September 2018
Available online 29 September 2018

Keywords:
Diffusion imaging
Non-Gaussian diffusion model
MRI
Obstructive sleep apnea
CPAP
Residual sleepiness

ABSTRACT

Objectives: To investigate factors associated with residual sleepiness in patients who were highly adherent to continuous positive airway pressure (CPAP). Nocturnal inactivity, comorbidities, concomitant medications, and, in particular, white matter (WM) differences using diffusion magnetic resonance imaging (MRI) were explored using a continuous-time random-walk (CTRW) model.

Methods: Twenty-seven male patients (30–55 years of age) with obstructive sleep apnea (OSA) received CPAP as the only treatment (CPAP $\geq$ 6 h/night) for at least 30 days. Based on the Psychomotor Vigilance Task (PVT) results, participants were divided into a non-sleepy group (lapses $\leq$ 5; $n = 18$) and a sleepy group (lapses > 5; $n = 9$). Mean nocturnal inactivity (sleep proxy) was measured using actigraphy for one week. Diffusion-weighted imaging (DWI) with high *b*-values, as well as diffusion tensor imaging (DTI), was performed on a 3 T MRI scanner. The DWI dataset was analyzed using the CTRW model that yielded three parameters: temporal diffusion heterogeneity α, spatial diffusion heterogeneity β, and an anomalous diffusion coefficient D_m. The differences in α, β, and D_m between the two groups were investigated by a whole-brain analysis using tract-based spatial statistics (TBSS), followed by a regional analysis on individual fiber tracts using a standard parcellation template. Results from the CTRW model were compared with those obtained from DTI. The three CTRW parameters were also correlated with the clinical assessment scores, Epworth Sleepiness Scale (ESS), PVT lapses, and PVT mean reaction time (MRT) in specific fiber tracts.

Results: There were no differences between groups in mean sleep duration, comorbidities, and the number or type of medications, including alerting and sedating medications. In the whole-brain DWI analysis, the sleepy group showed higher α (17.27% of the WM voxels) and D_m (17.14%) when compared to the non-sleepy group ($P < 0.05$), whereas no significant difference in β was observed. In the regional fiber analysis, the sleepy and non-sleepy groups showed significant differences in α, β, or their combinations in a total of 12 fiber tracts; whereas similar differences were not observed in DTI parameters, when age was used as a covariate. Additionally, moderate to strong correlations between the CTRW parameters (α,

Abbreviations: AD, axial diffusivity; CTRW, continuous-time random-walk; DTI, diffusion tensor imaging; DWI, diffusion-weighted imaging; FA, fractional anisotropy; FDR, false discovery rate; GM, gray matter; MD, mean diffusivity; MRI, magnetic resonance imaging; MRT, mean reaction time; RD, radial diffusivity; TBSS, tract-based spatial statistics; WM, white matter.

* Corresponding author. Center for Magnetic Resonance Research, University of Illinois at Chicago, 2242 West Harrison Street, Suite 103, MC 831, Chicago, IL, 60612, USA. Fax: +1312 355 1637.
** Corresponding author. College of Nursing, University of Illinois at Chicago, 845 S. Damen Avenue, M/C 802, Chicago, IL, 60612, USA. Fax: +1312 413 4399.
E-mail address: xjzhou@uic.edu (X.J. Zhou).
[1] XJZ and TEW are the senior authors who share the co-corresponding authorship.

https://doi.org/10.1016/j.sleep.2018.09.011

β, or D_m) and the sleepiness assessment scores (ESS, PVT lapses, or PVT MRT) were observed in specific fiber tracts ($|R| = 0.448–0.654$, $P = 0.0003–0.019$).
Conclusions: The observed differences in the CTRW parameters between the two groups indicate that WM alterations can be a possible mechanism to explain reversible versus residual sleepiness observed in OSA patients with identical high level of CPAP use. The moderate to strong correlations between the CTRW parameters and the clinical scores suggest the possibility of developing objective and quantitative imaging markers to complement clinical assessment of OSA patients.

1. Introduction

Obstructive sleep apnea (OSA), which affects 3–7% of adult men and 2–5% of adult women in the general population [1], is a chronic condition characterized by recurrent episodes of the upper-airway obstruction during sleep. It is categorized as mild, moderate, and severe on the basis of the apnea hypopnea index (AHI) [2]. This ventilatory disturbance can cause intermittent hypoxemia and sleep fragmentation, both of which are associated with multiple comorbidities in various systems [3,4]. Among these, OSA-related brain alterations have attracted increasing attention because of the central role of the brain in sleep-wake modulation [5].

Continuous positive airway pressure (CPAP) is a prevalent treatment strategy for OSA [6]. This device maintains airway patency during the night, eliminating breathing pauses in OSA patients. Effective treatment not only improves sleep quality, but also alleviates daytime somnolence and neurocognitive abnormalities [7–10]. Although the effectiveness of CPAP therapy has been widely demonstrated, it is noteworthy that this treatment fails in a substantial number of highly adherent patients [11]. In those using CPAP at least 6 h nightly, Weaver et al. documented that 34% of the patients manifested subjective sleepiness on the Epworth Sleepiness Scale (ESS), while 65% exhibited pathologic sleepiness on the Multiple Sleep Latency Test [10]. The underlying mechanism why only some patients respond to the treatment is poorly understood. Sleep duration may play a role, but documented on-mask use makes this explanation less likely. Of note, several studies have shown that long-term intermittent hypoxic exposure induces neuronal changes such as proinflammatory activation, reduced extracellular dopamine levels, increased oxidative stress, apoptosis, and gliosis in the brain regions associated with sleep-wake modulation [12–14]. These studies suggest that varying degrees of brain damage may be responsible for the differing responses among the OSA patients receiving comparable CPAP-treatment.

Recently, magnetic resonance imaging (MRI) was employed to investigate brain alterations associated with OSA. Although findings using conventional MRI were inconclusive [15], voxel-based morphometry showed reduced volume in some gray matter (GM) regions that were correlated with cognitive dysfunction of OSA patients [16]. More recently, magnetic resonance (MR) spectroscopy revealed changes of the hippocampus in OSA patients after CPAP-treatment [17]. In addition to GM, white matter (WM) alterations in OSA patients are equally important considering its pivotal role in neuronal signal transmission. Using diffusion tensor imaging (DTI) [18,19] with its two common parameters – fractional anisotropy (FA) and mean diffusivity (MD), Castronovo et al., reported significantly increased FA and decreased MD in multiple WM regions after CPAP-treatment [20]. However, the issue of why some patients remain somnolent with persistent CPAP adherence remains unclear. Using DTI with a tract-based spatial statistics (TBSS) analysis, Xiong et al., observed significant differences in MD and radial diffusivity (RD) between patients who did and did not manifest daytime hyper-somnolence with persistent CPAP use of greater than 6 h/night [21]. This suggests that varying degrees of WM damage in specific regions may explain why CPAP-treatment is effective only in some patients.

DTI is based upon a Gaussian diffusion model which typically employs a moderate b-value (eg, $b = 1000$ s/mm^2). As the b-value increases, diffusion in brain tissues exhibits non-Gaussian behavior that can be exploited using a variety of models to reveal the underlying tissue microstructures beyond what can be revealed by DTI. Examples of non-Gaussian diffusion models include stretched-exponential model, diffusion kurtosis imaging (DKI), continuous-time random-walk (CTRW) model, etc. [22–27], each focusing on different aspects of non-Gaussian characteristics. Among these models, the CTRW model has shown a unique capability for characterizing intravoxel tissue heterogeneity at high b-values [28,29], which may complement changes in MD and RD reported by Xiong et al. [21]. In this study, we employ a CTRW model combined with a TBSS [30] analysis to investigate possible tissue microstructural or heterogeneity differences between OSA patients with and without residual daytime sleepiness among those with comparable CPAP nightly use, thereby gaining additional insights into the mechanisms to explain the varying responses to CPAP therapy.

2. Materials and methods

2.1. Subjects

With approval of the Institutional Review Board and written informed consent, 27 male patients [age range: 30–55 years; mean age ± standard deviation (SD) = 44.1 ± 8.3 years] with OSA were enrolled in the study. The inclusion criteria were: (a) male with age between 30 and 55 years; (b) weight < 350 lbs with shoulder circumference ≤60 cm; (c) confirmed severe OSA by polysomnography (AHI ≥ 30 with oxygen desaturation > 5% at the time of treatment [31]); and (d) CPAP as the only treatment (CPAP ≥ 6 h/night for at least 30 days to allow for sufficient opportunity for resolution of excessive daytime sleepiness). The exclusion criteria were: (a) sleep disorders other than OSA; (b) night-shift workers; (c) history of brain injury or brain lesions observed on the acquired magnetic resonance images; or (d) contradictions to MRI (eg, MRI-incompatible implants, claustrophobia, etc.). The CPAP device employed in this study was equipped with a microprocessor that measures daily mask-on time and AHI along with technology to electronically transfer these data into a study database.

Psychomotor Vigilance Task (PVT) [32,33], an objective measure of daytime sleepiness, was conducted at the time of MRI scan. Based on the number of PVT lapses (defined as response time to a random stimulus > 500 ms) averaged between two measurements, the patients were divided into a non-sleepy group (ie, responders; PVT lapses ≤ 5; $n = 18$; age range = 30–55 years) and a sleepy group (ie, non-responders; PVT lapses > 5; $n = 9$; age range = 37–54 years). In addition to demographic variables, medications, comorbidities, body mass index (BMI), pre-CPAP AHI,

minimum oxygen saturation (Nadir SpO_2), and SpO_2 baseline were obtained during the initial interview and/or from the medical record. Mean nocturnal inactivity duration was determined using seven days of actigraphy and daily diary. Days of CPAP use in the past 30 days, mean CPAP pressure, and post-CPAP AHI were obtained from the CPAP device software. The ESS [34] and PVT were administered during the initial visit (~7–17 days before the MRI scan); and the PVT was also performed immediately prior to the MRI scan. In each PVT, both the PVT lapses and PVT mean reaction time (MRT) were recorded.

2.2. Image acquisition

The MRI examination consisted of axial T1-weighted 3D brain volume imaging (3D-BRAVO), sagittal T2-weighted 3D volume imaging (3D-CUBE), T2-weighted PROPELLER imaging, multi-*b*-value diffusion-weighted imaging (DWI), and DTI. All images were acquired on a 3 T MRI scanner (Discovery MR750, General Electric Health Care, Waukesha, WI) with a 32-channel head coil (Nova Medical Inc., Wilmington, MA). All the acquired MR images were examined to exclude possible lesions specified in the exclusion criteria by a neuroradiologist with eight years of experience. The multi-*b*-value DWI data were acquired with the following parameters: TR/TE = 4200/91.2 ms, FOV = 24 × 24 cm^2, matrix size = 256 × 256, pixel size = 0.94 × 0.94 mm^2, slice thickness = 3 mm, slice spacing = 1 mm, 14 b-values = 0_1, 10_1, 50_1, 100_1, 200_1, 400_1, 700_1, 1000_2, 1500_2, 2000_2, 2500_2, 3000_2, 3500_2, and 4000_2 s/mm^2 (the subscript indicates the number of averages), and the scan time = 4 min 20 s. At each non-zero *b*-value, trace-weighted images were obtained by applying the diffusion gradient successively along the three orthogonal directions in order to minimize the effect of diffusion anisotropy. The key DTI data acquisition parameters included: TR/TE = 4500/89.4 ms, FOV = 20 × 20 cm^2, matrix size = 256 × 256, pixel size = 0.78 × 0.78 mm^2, slice thickness = 3 mm, slice spacing = 1 mm, *b*-values = 0, 1000 s/mm^2, NEX = 1, gradient direction = 27, and the scan time = 8 min 29 s. The DTI images were used for WM segmentation in the TBSS analysis as described in the next sub-section.

2.3. Image analysis

The DTI dataset was employed to generate a common WM mask (or skeleton) among all participants to facilitate comparisons of the CTRW parameters obtained from the multi-*b*-value DWI dataset. To accomplish this, the DTI images were processed by FMRIB Software Library (FSL) [35] through the following steps: eddy current correction, BET brain extraction, DTIFIT reconstruction of diffusion tensors to produce FA maps, followed by a TBSS analysis. The images of all subjects were aligned to an FA standard template through a nonlinear co-registration. The aligned FA maps were then averaged to produce a skeleton highlighting the tracts common to the entire patient group.

In order to characterize the intravoxel tissue heterogeneities in the common WM fiber tracts that were determined by the TBSS analysis, the multi-*b*-value diffusion images were first co-registered among themselves, followed by an additional co-registration to the DTI images using the FMRIB's Linear Image Registration Tool (FLIRT). This approach helped mitigating image mis-registration errors caused by patient motion and/or eddy currents associated with different *b*-values. A CTRW model was then applied to the multi-*b*-value DWI dataset [29]. In the CTRW model, the diffusion-attenuated signal (S/S_0) is described by a Mittag-Leffler function, E_α:

$$\frac{S}{S_0} = E_\alpha\left[-(bD_m)^\beta\right] \quad (1)$$

where D_m is an anomalous diffusion coefficient, α and β correspond to temporal and spatial diffusion heterogeneity, respectively [29]. Using Eq. (1), the CTRW model was fitted to the multi-*b*-value diffusion images to produce α, β, and D_m maps.

Two WM analyses were performed on the multi-*b*-value DWI images co-registered to the DTI dataset. Firstly, a *whole-brain* analysis was carried out by projecting the α, β, and D_m maps of all subjects onto the FA skeleton, followed by an evaluation of CTRW parameter differences between the two patient groups, with age as a covariate, using the FSL permutation test with a statistical significance set at $P < 0.05$ (corrected with a threshold-free cluster enhancement or TFCE). Secondly, a *regional* WM analysis was performed using 1 mm JHU-ICBM labels [36] to produce 48 fiber tract regions of interest (ROIs). The average α, β, and D_m values within each ROI were computed and reported as mean ± SD. In addition, a binary logistic regression model was employed to evaluate the probability P_0 of using the combination of α and β to detect the statistical difference between the sleepy and non-sleepy groups:

$$P_0 = \frac{\exp(a_0 + a_1\alpha + a_2\beta)}{[1 + \exp(a_0 + a_1\alpha + a_2\beta)]} \quad (2)$$

where a_0 is a constant, and a_1 and a_2 are the regression coefficients for α and β, respectively. The regression coefficients were estimated by using a maximum-likelihood method [37]. To compare the CTRW results with those from DTI, the above two analyses were repeated on four DTI parameters: FA, MD, RD, and axial diffusivity (AD), each with a statistical significance set at $P < 0.05$.

2.4. Statistical analysis

Using SPSS 24.0 software (IBM, Armonk, NY), the demographics, physiological data, daytime sleepiness scores, nocturnal sleep duration, and CPAP-treatment metrics were first compared between the sleepy and non-sleepy groups using a Mann–Whitney U-test (Table 1a). Reported comorbidities were grouped into the following common categories: kidney transplant, cardiovascular diseases, diabetes mellitus, asthma, hypertension, hay-fever/seasonal allergies, and depression. The number of participants having a comorbidity in each group are listed in Table 1b where a Fisher's exact test was used to evaluate differences between the two groups. The median and interquartile range (IQR) for the number of medications, alerting medications, and sedating medications were also included in Table 1b. These quantities were compared using a Wilcoxon two-sample test with exact two-sided probability between the two patient groups.

Second, the average values of α, β, D_m, P_0, FA, MD, AD, and RD within an ROI for each patient group were obtained, followed by a comparison between the two groups using an analysis of covariance (ANCOVA), with age as a covariate, in the regional analysis described in the previous sub-section. After the *P*-values were obtained for the comparisons in each of the 48 fiber tracts, a Benjamin-Hochberg procedure was employed to perform false discovery rate (FDR) correction, producing the corrected *P*-values.

Lastly, possible correlations between the CTRW model parameters (α, β, and D_m) and clinical sleepiness scores were investigated in selected WM tracts by using a Pearson correlation analysis. In all statistical analyses, the statistical significance was set at $P < 0.05$.

Table 1a
Demographics and clinical characteristics of the patients.

Variables	Non-sleepy group (n = 18)	Sleepy group (n = 9)	*P*-value
Age (years)	43.1 ± 9.1	46 ± 6.4	0.527
Body Mass Index (kg/m^2)	33.2 ± 6.8	37.8 ± 4.6	0.076
Nocturnal sleep duration (hrs)	6.47 ± 0.79	6.10 ± 0.86	0.296
Nadir SpO_2 (%)	82.6 ± 11.3	83.1 ± 8.4	0.929
SpO_2 Baseline (%)	89.0 ± 7.9	90.6 ± 6.3	0.423
Days of CPAP use (>6 h/day)	29.1 ± 1.6	29.8 ± 0.7	0.143
Mean CPAP pressure (cmH_2O)	11.1 ± 4.5	12.9 ± 3.0	0.081
Pre-CPAP AHI	47.5 ± 34.7	58.7 ± 45.8	0.534
Post-CPAP AHI	3.3 ± 3.6	2.6 ± 2.4	0.916
Epworth Sleepiness Scale (ESS)	6.7 ± 4.7	8.8 ± 5.4	0.212
PVT lapses	1.7 ± 1.4	18.1 ± 25.1	<0.0001*
PVT mean reaction time (ms)	263.2 ± 29.2	395.3 ± 181.1	<0.0001*

Abbreviations: Apnea-Hypopnea Index (AHI); Psychomotor Vigilance Task (PVT). The raw data are expressed as mean ± standard deviation (SD). *P*-values were obtained from a Mann–Whitney U-test between the non-sleepy and sleepy groups with significant differences labeled by * (using $P < 0.05$ as a threshold).

Table 1b
Summary of patients' comorbidities and medications.

Variables	Non-sleepy group (n = 18)	Sleepy group (n = 9)	*P*-value
Kidney Transplant	1 (5.6)	2 (22.2)	0.2503
Cardiovascular	2 (11.1)	2 (22.2)	0.5818
Diabetes Mellitus	4 (22.2)	3 (33.3)	0.6527
Asthma	3 (16.7)	1 (11.1)	1
Hypertension	7 (38.9)	6 (66.7)	0.2365
Hay-fever/Seasonal Allergies	3 (16.7)	0 (0)	0.5292
Depression	6 (35.3)	2 (22.2)	0.6673
Median (IQR) Number of Medications	3 (5)	8 (9)	0.407
Median (IQR) Number of Alerting Medications	0 (2)	1 (2)	0.498
Median (IQR) Number of Sedating Medications	0.5 (1)	1 (2)	0.282

Cardiovascular diseases include heart failure, arrhythmia, left ventricular regurgitation, heart attack, and obstruction with four bypasses. The variable for comorbidities is expressed as "number (percentage)". The variable for medications is expressed as "median number (IQR number)". IQR: interquartile range.
The *P*-values for comorbidities and medications were calculated from a Fisher's exact test and a Wilcoxon two-sample test with exact two-sided probability, respectively. *P*-value < 0.05 was considered statistically significant.

3. Results

3.1. Demographic and clinical data

As summarized in Table 1a, no significant difference in age, BMI, nocturnal sleep duration, nadir SpO_2, SpO_2 baseline, days of CPAP use in the past 30 days, mean CPAP pressure, pre-CPAP AHI, post-CPAP AHI, or post-CPAP ESS was observed between the sleepy and non-sleepy groups ($P > 0.05$). The mean nocturnal sleep duration for either group was consistent with the average sleep duration of most normal individuals in the US [38]. However, the post-CPAP PVT lapses and MRT were significantly different ($P < 0.05$). Table 1b shows no significant difference between the two groups ($P > 0.05$) in comorbidities, including kidney transplant, cardiovascular diseases, diabetes mellitus, asthma, hypertension, hay-fever/seasonal allergies, depression, as well as the numbers of medications, alerting medications, and sedating medications.

3.2. Whole-brain comparison of diffusion parameters

In the whole-brain analysis based on the CTRW parameters, the OSA patients with residual sleepiness showed a higher α in 17.27% (23,810/137,832 voxels) and D_m in 17.14% (23,627/137,832 voxels) of the WM skeletons when compared to the non-sleepy subjects ($P < 0.05$) (Fig. 1a), whereas no significant difference in β was observed ($P > 0.05$). Differences in α and D_m were mostly observed in the bilateral corona radiate (CR), external capsule (EC), superior longitudinal fasciculus (SLF), corpus callosum (CC), right sagittal stratum (SS.R), and right internal capsule (IC.R).

In the whole-brain analysis based on the DTI parameters, patients in the sleepy group showed a higher MD in 9.69% (13,358/137,832 voxels) and RD in 12.75% (17,580/137,832 voxels) of the WM skeletons when compared with the non-sleepy subjects ($P < 0.05$). No significant difference in FA or AD was observed ($P > 0.05$) (Fig. 1b).

3.3. Regional comparison in specific fiber tracts between the groups

Figs. 2 and 3 summarize the results from the regional fiber analysis, illustrating the individual fiber tracts that exhibited significant difference ($P < 0.05$) in α and β, respectively. The sleepy group showed a higher α than the non-sleepy group in a total of four fiber tracts (Fig. 2), and a lower β in the body of corpus callosum (BCC) and right superior longitudinal fasciculus (SLF.R) (Fig. 3). With the combination of α and β parameters, P_0 exhibited significant difference in a total of twelve fiber tracts, as summarized in Table 2. All the *P*-values shown in Figs. 2 and 3, and Table 2 were FDR-corrected with age as a covariate. Without FDR correction, the sleepy group exhibited a significantly higher D_m value than the non-sleepy group ($P < 0.05$) in twelve fiber tracts (Fig. 4). In the regional analysis with age as a covariate, however, none of the DTI parameters (FA, MD, RD, and AD) exhibited a significant difference with FDR-corrected $P > 0.05$.

3.4. Correlations between CTRW model parameters and sleepiness assessment scores

The correlations between the CTRW parameters (α, β, or D_m) and the sleepiness assessment scores (ESS, PVT lapses, or PVT MRT) in specific fiber tracts are shown in Fig. 5. The average CTRW values were derived from the ROI on the tract within the entire skeleton determined from the TBSS analysis. The results indicated that α and D_m were positively correlated with ESS [α in the right superior fronto-occipital fasciculus (SFO.L): $R = 0.634$, $P = 0.0003$; D_m in the right corticospinal tract (CST.R): $R = 0.448$, $P = 0.019$], PVT lapses [α: $R = 0.493$, $P = 0.009$; and D_m: $R = 0.446$, $P = 0.019$; both in the right superior corona radiata (SCR.R)], and PVT MRT [(α: $R = 0.511$, $P = 0.007$; and D_m: $R = 0.49$, $P = 0.009$; both in SCR.R)], while β was negatively correlated with the ESS ($R = -0.514$, $P = 0.006$; in CST.R), PVT lapses ($R = -0.654$, $P = 0.0002$; in SCR.R), and PVT MRT ($R = -0.644$, $P = 0.0003$, in SCR.R).

4. Discussion

In this study on participants with high levels of CPAP use, we did not find that nocturnal sleep duration, residual on-treatment AHI, age, BMI, nadir SpO_2 (%), SpO_2 baseline (%), comorbidities or medications contributed to the differences between those with and without objectively measured excessive daytime sleepiness. Although there were differences in PVT lapses (by group definition)

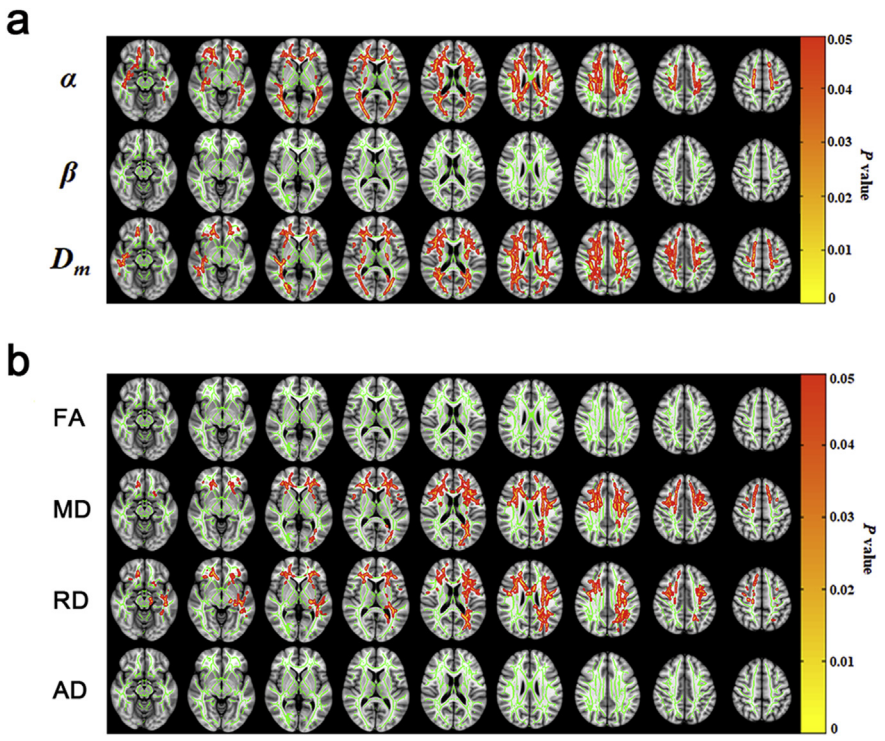

Fig. 1. **(a)** Whole-brain α, β, and D_m maps showing the presence or absence of differences between the sleepy and non-sleepy groups. **(b)** Results from the DTI whole-brain analysis based on FA, MD, RD, and AD maps showing the presence or absence of differences between the sleepy and non-sleepy groups. Age was included as a covariate in the group analyses for all parameters. Green: mean fractional anisotropy (FA) skeleton (threshold = 0.2) without significant change. Red-yellow: voxels with significantly increased parameter values in the sleepy group as compared to the non-sleepy group with *P*-value < 0.05 as shown in the color bar. (For interpretation of the references to color in this figure legend, the reader is referred to the Web version of this article.)

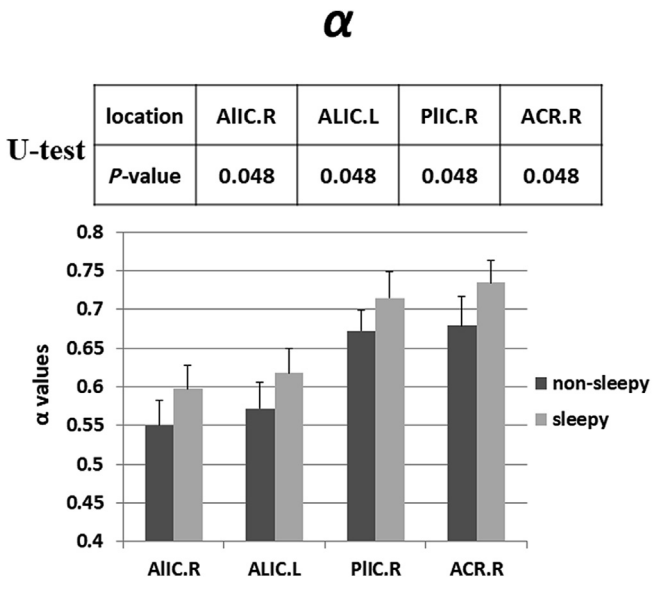

Fig. 2. Fiber tracts showing a significantly higher α value in the sleepy group as compared to the non-sleepy group. The inset table summarizes the *P*-values of fiber tracts in which the two patient groups exhibited significant difference in α values (FDR-corrected $P < 0.05$). The abbreviations of WM fiber tracts are as following: anterior limb of right and left internal capsule (ALIC.R and ALIC.L, respectively), posterior limb of right internal capsule (PLIC.R), and right anterior corona radiata (ACR.R).

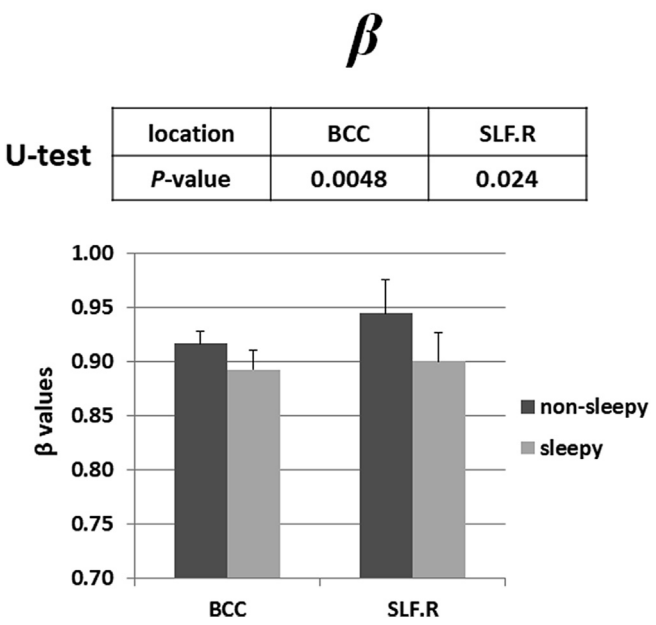

Fig. 3. Fiber tracts showing a significantly lower β value in the sleepy group as compared to the non-sleepy group. The inset table summarizes the *P*-values of fiber tracts in which the two patient groups exhibited significant difference in β values (FDR-corrected $P < 0.05$). The abbreviations of WM fiber tracts are as following: body of corpus callosum (BCC) and right superior longitudinal fasciculus (SLF.R).

and mean reaction time indicating an effect on neurobehavioral performance, it is noteworthy that there were no statistically reliable differences in self-reported sleepiness (ESS scores) between the two groups, which may be attributed to the small sample size. However, the inability of individuals to recognize their daytime sleepiness, especially with chronic manifestation, has been previously reported [39], which may account for the lack of perception in the sleepy group.

Table 2
Fiber tracts showing differences between the two groups as measured by P_0.

Fiber	Non-sleepy	Sleepy	*P*-value
CP.R	0.172 ± 0.209	0.655 ± 0.313	0.0024
CP.L	0.183 ± 0.203	0.633 ± 0.336	0.0016
RLIC.L	0.190 ± 0.167	0.619 ± 0.323	0.0008
FX.R	0.240 ± 0.219	0.521 ± 0.229	0.0340
ALIC.R	0.152 ± 0.233	0.697 ± 0.289	0.0012
ALIC.L	0.217 ± 0.232	0.567 ± 0.259	0.0160
PLIC.R	0.167 ± 0.249	0.667 ± 0.257	0.0010
PLIC.L	0.247 ± 0.154	0.505 ± 0.285	0.0380
ACR.R	0.185 ± 0.224	0.631 ± 0.262	0.0007
SLF.R	0.172 ± 0.228	0.657 ± 0.282	0.0006
BCC	0.178 ± 0.191	0.645 ± 0.300	0.0048
UNC.R	0.264 ± 0.158	0.473 ± 0.258	0.0480

Abbreviations: CP: cerebral peduncle; RLIC: retrolenticular part of internal capsule; FX: fornix; ALIC: anterior limb of internal capsule; PLIC: posterior limb of internal capsule; ACR: anterior corona radiata; SLF: superior longitudinal fasciculus; BCC: body of corpus callosum; UNC: uncinate fasciculus. '.R' denotes right, and '.L' left. P_0 represents a probability of the combination of α and β, and is expressed as mean ± standard deviation (SD). *P*-values showing the difference between the non-sleepy and sleepy groups were obtained by an analysis of covariance (ANCOVA), with age as a covariate.

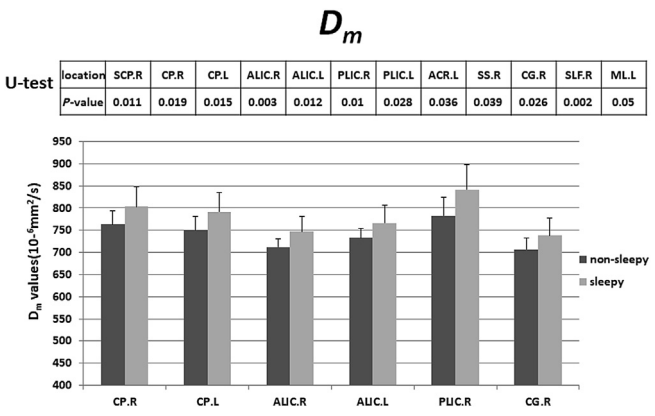

Fig. 4. Selected six fiber tracts showing a significantly higher D_m value in the sleepy group as compared to the non-sleepy group. The inset table summarizes the *P*-values of all twelve fiber tracts in which the two patient groups exhibited significant difference in D_m values ($P < 0.05$) without FDR-correction. The abbreviations of WM fiber tracts are as following: right superior cerebellar peduncle (SCP.R), right and left cerebral peduncle (CP.R and CP.L, respectively), anterior limb of right and left internal capsule (ALIC.R and ALIC.L, respectively), posterior limb of right and left internal capsule (PLIC.R and PLIC.L, respectively), left anterior corona radiata (ACR.L), right Sagittal striatum (SS.R), right cingulum (CG.R), right superior longitudinal fasciculus (SLF.R), and left medial lemniscus (ML.L).

Using an advanced non-Gaussian diffusion model – the CTRW model – that is sensitive to tissue microstructure and heterogeneity, we observed significantly different α, β, and D_m values in WM, globally and/or regionally, between the sleepy and non-sleepy OSA patients with comparable CPAP-treatment. The whole-brain analysis and regional analysis focused on voxels and ROIs, respectively, complementing each other in detecting the observed differences. Since the CTRW parameters reflect the underlying tissue structures or heterogeneities [29,40], the observed differences in these parameters between the two patient groups suggest that brain WM alterations can be likely a mechanism to explain reversed versus residual sleepiness among OSA patients with similar CPAP nightly use.

In OSA, it is well known that intermittent hypoxia can lead to oxidative stress and ischemia-reperfusion injury [41] in the entire brain including both GM and WM. Although neurons in GM are more susceptible to hypoxic insult than glial cells in WM due to their higher oxygen consumption [42], WM is also subject to such insult as its blood supply is provided by perforating arteries lacking of anastomosis and effective collateral circulation [43]. The compromised WM may or may not be recoverable during the course of CPAP-treatment, explaining why OSA patients may respond differently. WM recovery in OSA patients was reported by Castronovo et al., [20] who observed an increase in FA and a decrease in MD in some WM regions throughout the course of CPAP-treatment. Both of these changes are indications of improved WM integrity in selected areas that are associated with the recovery. Very recently, Xiong et al., observed significant differences in MD and RD between patients with and without somnolence following similar CPAP-treatment [21], indicating that the WM damage in specific regions may not recover quickly, or may not recover at all, despite persistent CPAP-treatment. In this study, we also observed significant differences in MD and RD in the whole-brain analysis, but to a lesser extent than what was reported by Xiong et al., [21] In addition, the differences in MD and RD diminished in our regional analysis. These discrepancies as compared to the report [21] were most likely due to the fact that age was included as a covariate in our study to improve its scientific rigor. It is significant to note that the CTRW non-Gaussian diffusion parameters exhibited differences in both whole-brain and regional analyses even with the inclusion of age as a covariate. Moreover, the extent of the affected tracts revealed by the CTRW parameters (α and D_m) was considerably larger than that by the DTI parameters (MD and RD) in the whole brain analysis (Fig. 1). These results strongly indicate that the CTRW parameters can be more sensitive than the conventional DTI parameters to the WM differences between the two OSA patient groups.

In the CTRW diffusion model [29], α has been associated with temporal diffusion heterogeneity, which describes the likelihood of water molecules to be trapped or released when they are diffusing through a complex tissue structure, leading to a variable time for each move. When α approaches to 1, the diffusion time for each move corresponds to a Gaussian distribution. The degree of deviation from 1 indicates an increased temporal diffusion heterogeneity in biological tissues [29]. Hypoxia and/or ischemia associated with OSA can result in degeneration or even cell death of neurons and oligodendrocytes, which eventually leads to shrinkage of axons and myelin sheaths [44]. This in turn can lead to a temporally more homogeneous environment for the diffusing water molecules of being trapped or released throughout the diffusion process, explaining the elevated α value in both whole-brain and regional analyses observed in our study.

Complementary to α, β has been related to spatial diffusion heterogeneity [25,29,45,46], which describes the heterogeneous nature of diffusion "jump" length in each move and is independent of diffusion coefficient [25,47]. In a homogeneous medium in which the jump length follows a Gaussian distribution, β equals 1. A decrease in β from 1 indicates increased tissue structural heterogeneity. An episode of intermittent hypoxia-ischemia can cause different degrees of damage to oligodendrocytes – the myelin-forming cells [44], leading to a compromised myelin sheath and a spatially more heterogeneous diffusion environment (ie, a decreased β in the sleepy group as we observed in the regional analysis). Once these cells are severely damaged by hypoxia-ischemia, the OSA patients may continue showing sleepiness despite persistent CPAP therapy. Other factors can also contribute to the increase in spatial heterogeneity. For example, hypoxic exposure can trigger inflammatory reaction to produce a multitude of inflammatory cells [41], which increases the complexity of the environment. It is important to recognize that spatial diffusion heterogeneity and temporal diffusion heterogeneity are independent from and complementary to each other, as we observed in our

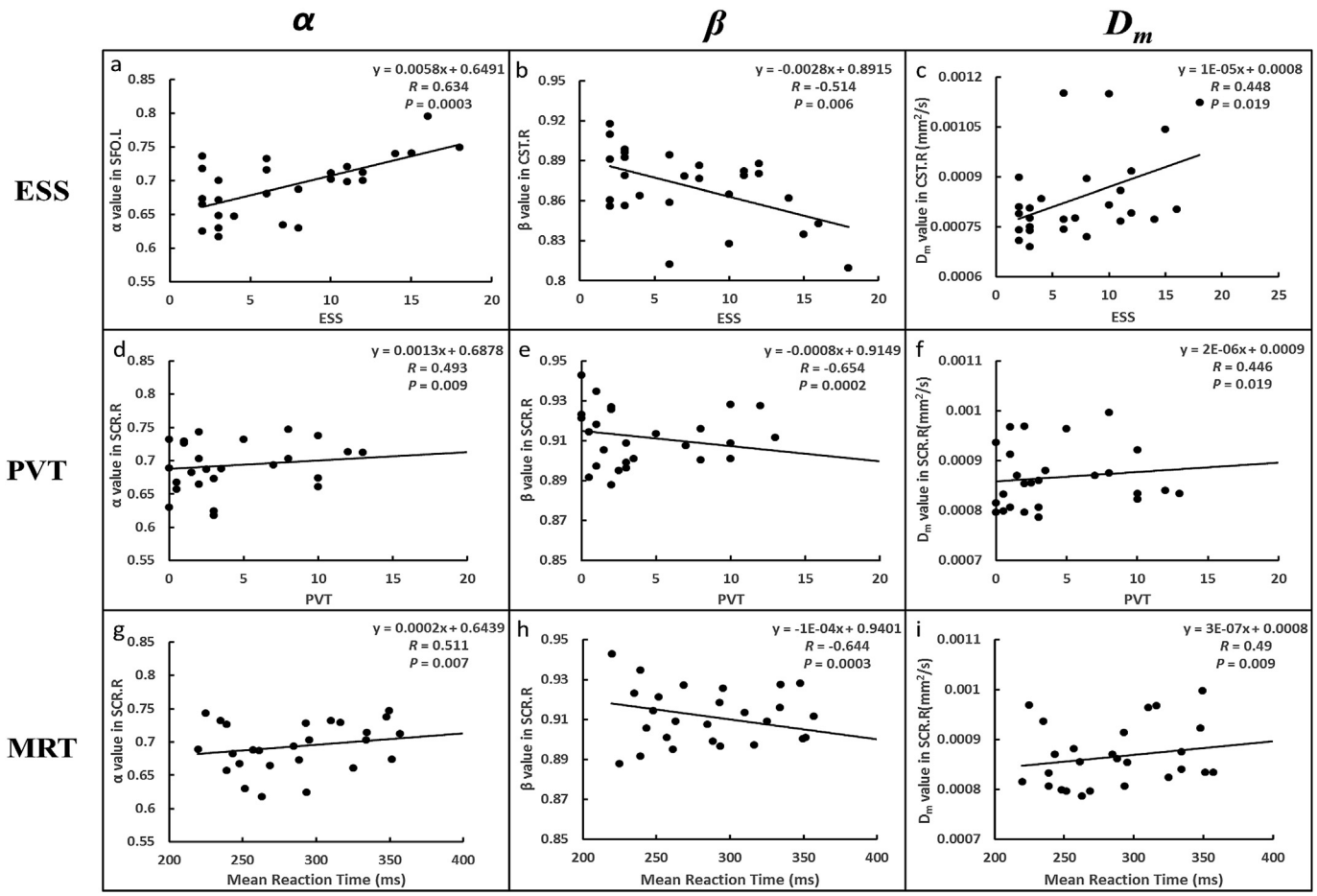

Fig. 5. Correlations between CTRW parameters [α (a,d,g), β (b,e,h), and D_m (c,f,i)] and clinical assessment scores [ESS (a,b,c), PVT lapses (d,e,f), and PVT MRT (g,h,i)] in specific fiber tracts as indicated along the vertical axes. The linear regression equation, Pearson correlation coefficient (R) and the P-value are shown in each plot. Abbreviations: ESS: Epworth Sleepiness Scale; PVT: Psychomotor Vigilance Task; MRT: mean reaction time.

study. The complementary nature allows us to probe the microscopic tissue environment from two different angles, which is a considerable advantage offered by the CTRW diffusion model. This advantage was exploited in this study by considering α and β jointly, as represented by P_0 (Table 2).

The anomalous diffusion coefficient, D_m, is analogous to apparent diffusion coefficient (ADC) or MD. Although the regional fiber analysis did not show significant difference in D_m after FDR correction, a significantly higher D_m was observed in the sleepy group without FDR correction (Fig. 4). In addition, the whole-brain analysis also demonstrated that the sleepy group had a higher D_m value with statistical significance (Fig. 1a). The increased D_m is consistent with the elevated MD observed in this study as well as previous reports [21]. This can be attributed to the more extensive shrinkage of axons and myelin, leading to an increase in extracellular space [48], and/or hypoxia-related vascular injury [49] in the sleepy group as compared to the non-sleepy group.

The compromised WM fiber tracts observed in this study reside in autonomic or respiratory control regions (insular cortices, midline pons, cerebellar peduncles, and cerebellar vermis), as well as in neuropsychologic, motor, or cognitive regulatory areas (hippocampus, amygdala, internal and external capsules, ventral putamen, frontal, parietal, and temporal white matter regions), all of which are relevant to OSA [50]. For example, the corona radiata propagates from the frontal/parietal cortex to the brain stem via internal capsule, which involves a number of fiber tracts (eg, ACR.R, ALIC.R, PLIC.R, ALIC.L). Any compromise to these fiber tracts could slow neuronal transmission, affecting the sleep-wake modulation. Although the exact mechanism of how these fiber tracts affect somnolence remains unclear, the results from our study provide new motivations for further investigations.

In addition to providing evidence showing that the underlying WM microstructural change can be a possible explanation why only some patients respond to CPAP-treatment, our study also demonstrates moderate to strong correlations between the CTRW diffusion parameters and clinical scores for evaluating somnolence. These correlations suggest that the WM structural alterations can be a continuous process in OSA patients. Given the limited sample size, we did not intend to establish a threshold for α, β, or D_m value to separate reversible versus residual sleepiness. However, our results indicate a possibility for developing imaging-based, objective, quantitative markers to complement the conventional scores used clinically.

Based on a report that white matter undergoes degenerative changes with normal aging [51], we performed our statistical analysis by taking age as a covariate to improve the scientific rigor. Further improvement may also be achieved by including BMI as another covariate. Like several other recent imaging studies on OSA [5,50,52], the present study did not include BMI as a covariate because of the following reasons. First, although individuals with higher BMI tend to have a higher prevalence of OSA, WM change affected by BMI has not been fully established in the literature,

despite recent reports on a limited number of tracts [53,54]. Second, no significant difference in BMI was observed between the sleepy and non-sleepy groups as reported in Table 1a. Third, the BMI of some study subjects fluctuated noticeably, introducing an additional complexity if BMI were included in a covariate.

Our study has additional limitations. First, the study design was cross-sectional without pre-treatment MRI scans. However, all our subjects had chronic severe OSA (AHI $\geq$ 30 with oxygen desaturation > 5% at the time of treatment), partially justifying the assumption that the pre-treatment baseline MRI data were similar. In addition, the clinical characteristics (Table 1a) and comorbidities (Table 1b) showed no significant difference between the sleepy and non-sleepy groups. Foremost, however, is the inability to determine who would be adherent to CPAP treatment prior to therapy, especially given the high rate of non-adherence of approximately 50%. Second, only male patients were included to eliminate the potential gender differences. As such, the observations may not be extended to the general population. Third, a normal control group was not included in this study. The data of normal subjects would provide a more reliable reference for determining WM abnormality. Lastly, the sample size may have produced a Type II error for finding differences between groups for putative variables explored aside from the imaging metrics.

5. Conclusions

Using a novel non-Gaussian diffusion model – the CTRW model – and a TBSS analysis, we have observed significant differences in WM both globally and regionally between the somnolent and non-somnolent OSA patients with high level of CPAP use. The differences observed in the CTRW parameters support the hypothesis that varying degrees of WM injury in OSA patients can be responsible for the lack of response to CPAP-treatment. The value of the CTRW parameters is further illustrated through their moderate to strong correlations with several commonly used sleepiness assessment scores, suggesting a possibility of using these objective imaging-based parameters to complement clinical assessment. Moreover, the CTRW parameters have exhibited better sensitivity to the WM differences than the DTI metrics. Taken together, these new findings are expected to help understanding brain damage related to OSA and guiding the development of effective therapies.

Acknowledgments

This work was supported by an investigator-initiated grant from TEVA Pharmaceuticals, Inc. (TEW), grants from the US National Institutes of Health (1S10RR028898 and 1R01EB026716; XJZ), and a fellowship from China Scholarship Council (JZ). We thank Hagai Ganin for technical assistance, Drs. Yi Sui, Kejia Cai, Rongwen Tain, and Liping Qi for valuable discussions, Dr. Robert DiDomenico for generating the scheme and classifying medications, and Dr. Aiman Tulaimat of John H. Stroger Hospital of Cook County for patient recruitment.

Conflicts of interest

The ICMJE Uniform Disclosure Form for Potential Conflicts of Interest associated with this article can be viewed by clicking on the following link: https://doi.org/10.1016/j.sleep.2018.09.011.

References

[1] Punjabi NM. The epidemiology of adult obstructive sleep apnea. Proc Am Thorac Soc 2008;5:136–43.
[2] Senaratna CV, Perret JL, Lodge CJ, et al. Prevalence of obstructive sleep apnea in the general population: a systematic review. Sleep Med Rev 2017;34:70–81.
[3] Kang EW, Abdel-Kader K, Yabes J, et al. Association of sleep-disordered breathing with cognitive dysfunction in CKD stages 4-5. Am J Kidney Dis 2012;60:949–58.
[4] Bradley TD, Floras JS. Obstructive sleep apnoea and its cardiovascular consequences. Lancet 2009;373:82–93.
[5] Macey PM, Kumar R, Woo MA, et al. Brain structural changes in obstructive sleep apnea. Sleep 2008;31:967–77.
[6] McDaid C, Durée KH, Griffin SC, et al. A systematic review of continuous positive airway pressure for obstructive sleep apnoea-hypopnoea syndrome. Sleep Med Rev 2009;13:427–36.
[7] Antic NA, Catcheside P, Buchan C, et al. The effect of CPAP in normalizing daytime sleepiness, quality of life, and neurocognitive function in patients with moderate to severe OSA. Sleep 2011;34:111–9.
[8] Donovan LM, Boeder S, Malhotra A, et al. New developments in the use of positive airway pressure for obstructive sleep apnea. J Thorac Dis 2015;7:1323–42.
[9] Aurora RN, Collop NA, Jacobowitz O, et al. Quality measures for the care of adult patients with obstructive sleep apnea. J Clin Sleep Med 2015;11:357–83.
[10] Weaver TE, Maislin G, Dinges DF, et al. Relationship between hours of CPAP use and achieving normal levels of sleepiness and daily functioning. Sleep 2007;30:711–9.
[11] Gasa M, Tamisier R, Launois SH, et al. Residual sleepiness in sleep apnea patients treated by continuous positive airway pressure. J Sleep Res 2013;22:389–97.
[12] Alchanatis M, Deligiorgis N, Zias N, et al. Frontal brain lobe impairment in obstructive sleep apnoea: a proton MR spectroscopy study. Eur Respir J 2004;24:980–6.
[13] Vernet C, Redolfi S, Attali V, et al. Residual sleepiness in obstructive sleep apnoea: phenotype and related symptoms. Eur Respir J 2011;38:98–105.
[14] Veasey SC, Davis CW, Fenik P, et al. Long-term intermittent hypoxia in mice: protracted hypersomnolence with oxidative injury to sleep-wake brain regions. Sleep 2004;27:194–201.
[15] Zimmemnan ME, Aloia MS. A review of neuroimaging in obstructive sleep apnea. J Clin Sleep Med 2006;2:461–71.
[16] Macey PM, Henderson LA, Macey KE, et al. Brain morphology associated with obstructive sleep apnea. Am J Respir Crit Care Med 2002;166:1382–7.
[17] Kızılgöz V, Aydın H, Tatar IG, et al. Proton magnetic resonance spectroscopy of periventricular white matter and hippocampus in obstructive sleep apnea patients. Pol J Radiol 2013;78:7–14.
[18] Kumar R, Pham TT, Macey PM, et al. Abnormal myelin and axonal integrity in recently diagnosed patients with obstructive sleep apnea. Sleep 2014;37:723–32.
[19] Chen HL, Lu CH, Lin HC, et al. White matter damage and systemic inflammation in obstructive sleep apnea. Sleep 2015;38:361–70.
[20] Castronovo V, Scifo P, Castellano A, et al. White matter integrity in obstructive sleep apnea before and after treatment. Sleep 2014;37:1465–75.
[21] Xiong Y, Zhou XJ, Nisi RA, et al. Brain white matter changes in CPAP-treated obstructive sleep apnea patients with residual sleepiness. J Magn Reson Imag 2017;45:1371–8.
[22] Niendorf T, Dijkhuizen RM, Norris DG, et al. Biexponential diffusion attenuation in various states of brain tissue: implications for diffusion-weighted imaging. Magn Reson Med 1996;36:847–57.
[23] Bennett KM, Schmainda KM, Bennett R, et al. Characterization of continuously distributed cortical water diffusion rates with a stretched-exponential model. Magn Reson Med 2003;50:727–34.
[24] Jensen JH, Helpern JA, Ramani A, et al. Diffusional kurtosis imaging: the quantification of non-Gaussian water diffusion by means of magnetic resonance imaging. Magn Reson Med 2005;53:1432–40.
[25] Sui Y, Wang H, Liu G, et al. Differentiation of low- and high-grade pediatric brain tumors with high b-value diffusion-weighted MR imaging and a fractional order calculus model. Radiology 2015;277:489–96.
[26] Karaman MM, Wang H, Sui Y, et al. A fractional motion diffusion model for grading pediatric brain tumors. Neuroimage Clin 2016;12:707–14.
[27] Zhang H, Schneider T, Wheeler-Kingshott CA, et al. NODDI: practical in vivo neurite orientation dispersion and density imaging of the human brain. Neuroimage 2012;61:1000–16.
[28] Ingo C, Magin RL, Colon-Perez L, et al. On random walks and entropy in diffusion-weighted magnetic resonance imaging studies of neural tissue. Magn Reson Med 2014;71:617–27.
[29] Karaman MM, Sui Y, Wang H, et al. Differentiating low- and high-grade pediatric brain tumors using a continuous-time random-walk diffusion model at high b-values. Magn Reson Med 2015;76:1149–57.
[30] Smith SM, Jenkinson M, Johansen-Berg H, et al. Tract-based spatial statistics: voxelwise analysis of multi-subject diffusion data. Neuroimage 2006;31:1487–505.
[31] Ruehland WR, Rochford PD, O'Donoghue FJ, et al. The new AASM criteria for scoring hypopneas: impact on the apnea hypopnea index. Sleep 2009;32:150–7.
[32] Basner M, Dinges DF. Maximizing sensitivity of the psychomotor vigilance test (PVT) to sleep loss. Sleep 2011;34:581–91.

[33] Batool-Anwar S, Kales SN, Patel SR, et al. Obstructive sleep apnea and psychomotor vigilance task performance. Nat Sci Sleep 2014;6:65–71.
[34] Johns MW. A new method for measuring daytime sleepiness: the Epworth sleepiness scale. Sleep 1991;14:540–5.
[35] Jenkinson M, Beckmann CF, Behrens TEJ, et al. FSL. Neuroimage 2012;62:782–90.
[36] Mori S, Oishi K, Jiang H, et al. Stereotaxic white matter atlas based on diffusion tensor imaging in an ICBM template. Neuroimage 2008;40:570–82.
[37] Menard S. Applied logistic regression analysis. Sage; 2002. p. 1–120.
[38] Dijk DJ, Groeger JA, Stanley N, et al. Age-related reduction in daytime sleep propensity and nocturnal slow wave sleep. Sleep 2010;33:211–23.
[39] Van Dongen HPA, Maislin G, Mullington JM, et al. The cumulative cost of additional wakefulness: dose-response effects on neurobehavioral functions and sleep physiology from chronic sleep restriction and total sleep deprivation. Sleep 2003;26:117–26.
[40] Xiong Y, Sui Y, Xie KL, et al. Differentiation of low- and high-grade gliomas using high b-value diffusion imaging with a non-Gaussian diffusion model. Am J Neuroradiol 2016;37:1643–9.
[41] Jelic S, Padeletti M, Kawut SM, et al. Inflammation, oxidative stress, and repair capacity of the vascular endothelium in obstructive sleep apnea. Circulation 2008;117:2270–8.
[42] Dirnagl U, Iadecola C, Moskowitz MA. Pathobiology of ischaemic stroke: an integrated view. Trends Neurosci 1999;22:391–7.
[43] Brown WR, Thore CR. Review: cerebral microvascular pathology in ageing and neurodegeneration. Neuropathol Appl Neurobiol 2011;37:56–74.
[44] Mifsud G, Zammit C, Muscat R, et al. Oligodendrocyte pathophysiology and treatment strategies in cerebral ischemia. CNS Neurosci Ther 2014;20:1–10.
[45] Kwee TC, Galbán CJ, Tsien C, et al. Intravoxel water diffusion heterogeneity imaging of human high-grade gliomas. NMR Biomed 2010;23:179–87.
[46] Tang L, Sui Y, Zhong Z, et al. Non-Gaussian diffusion imaging with a fractional order calculus model to predict response of gastrointestinal stromal tumor to second-line sunitinib therapy. Magn Reson Med 2018;79:1399–406.
[47] Zhou XJ, Gao Q, Abdullah O, et al. Studies of anomalous diffusion in the human brain using fractional order calculus. Magn Reson Med 2010;63:562–9.
[48] Kumar R, Chavez AS, Macey PM, et al. Altered global and regional brain mean diffusivity in patients with obstructive sleep apnea. J Neurosci Res 2012;90:2043–52.
[49] Yadav SK, Kumar R, Macey PM, et al. Regional cerebral blood flow alterations in obstructive sleep apnea. Neurosci Lett 2013;555:159–64.
[50] Tummala S, Roy B, Vig R, et al. Non-Gaussian diffusion imaging shows brain myelin and axonal changes in obstructive sleep apnea. J Comput Assist Tomogr 2017;41:181–9.
[51] Salat DH, Tuch DS, Greve DN, et al. Age-related alterations in white matter microstructure measured by diffusion tensor imaging. Neurobiol Aging 2005;26:1215–27.
[52] Tummala S, Palomares J, Kang DW, et al. Global and regional brain non-Gaussian diffusion changes in newly diagnosed patients with obstructive sleep apnea. Sleep 2016;39:51–7.
[53] Kullmann S, Callaghan MF, Heni M, et al. Specific white matter tissue microstructure changes associated with obesity. Neuroimage 2016;125:36–44.
[54] Bolzenius J, Laidlaw D, Cabeen R, et al. Brain structure and cognitive correlates of body mass index in healthy older adults. Behav Brain Res 2015;278:342–7.